

This file includes:

Table S1

Figures S1 to S10

Table S1. Case studies used for WRF simulation. The daily mean cloud liquid water path (LWP), cloud condensation nuclei (CCN) concentration, synoptic regime classification and cloud-state classification are listed for each case.

Date	LWP (g m ⁻²)	CCN (cm ⁻³)	Synoptic	Cloud state
2016-07-01	219.8	91.1	High_Ridge	Precipitating
2016-07-21	109.3	244.2	High_Ridge	Precipitating to non-precipitating thick
2016-07-22	52.2	399.3	High_Ridge	Non-precipitating thin
2016-07-25	85.5	121.3	High_Ridge	Precipitating
2016-07-28	64.8	357.9	High_Ridge	Non-precipitating thin
2017-07-06	52.0	265.4	High_Ridge	Non-precipitating thin
2017-07-18	112.1	91.7	Post trough	Non precipitating thick
2017-07-19	158.2	117.5	Post trough	Non precipitating thick to Precipitating
2017-07-20	230.7	186.6	High_Ridge	Non precipitating thick
2017-08-26	139.2	270.7	Post trough	Non-precipitating thick
2019-08-23	161.7	86.5	Weak trough	Precipitating to non-precipitating thick

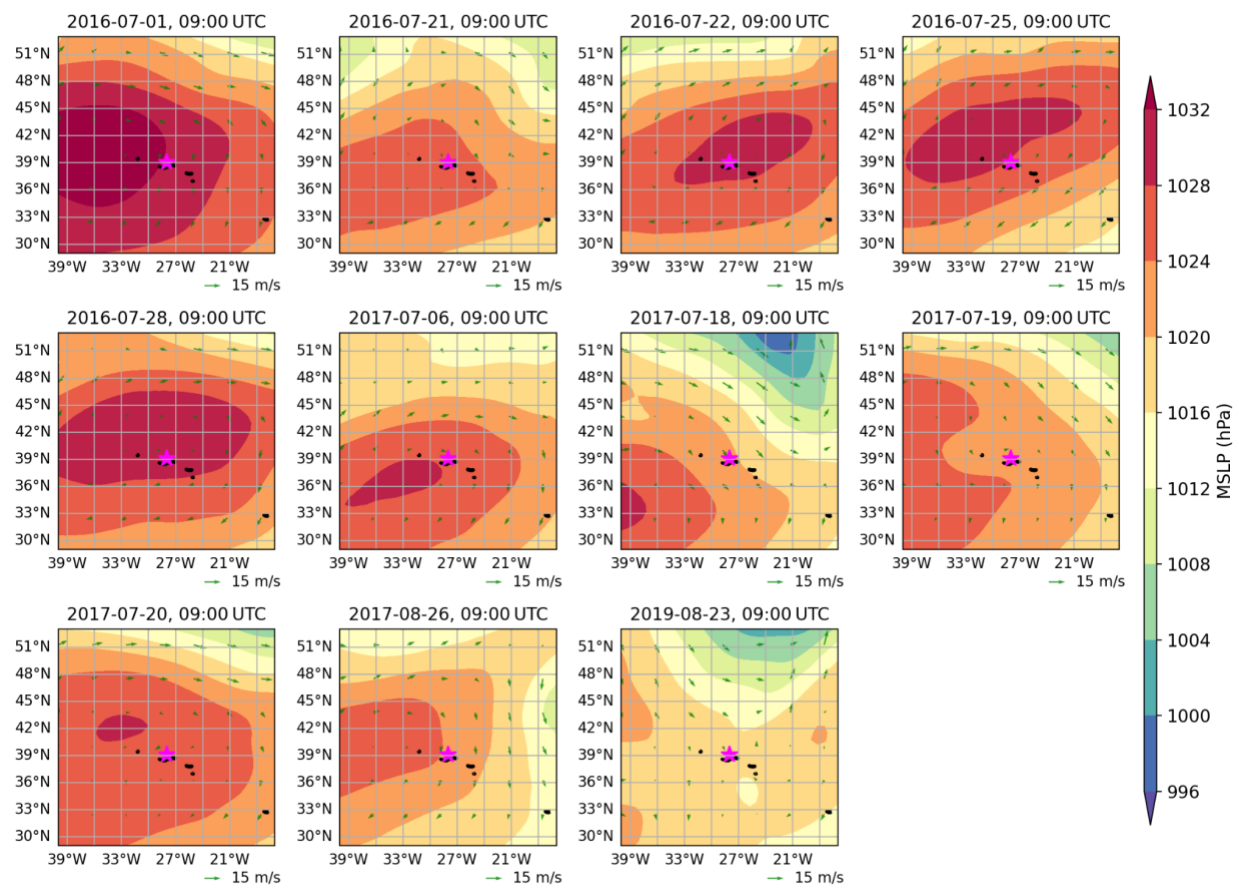


Figure S1. Mean sea-level pressure (MSLP, contour; units: hPa) and 10-m surface wind vectors (arrows; units: m s^{-1}) from ERA5 reanalysis at 09:00 UTC for all 11 cases.

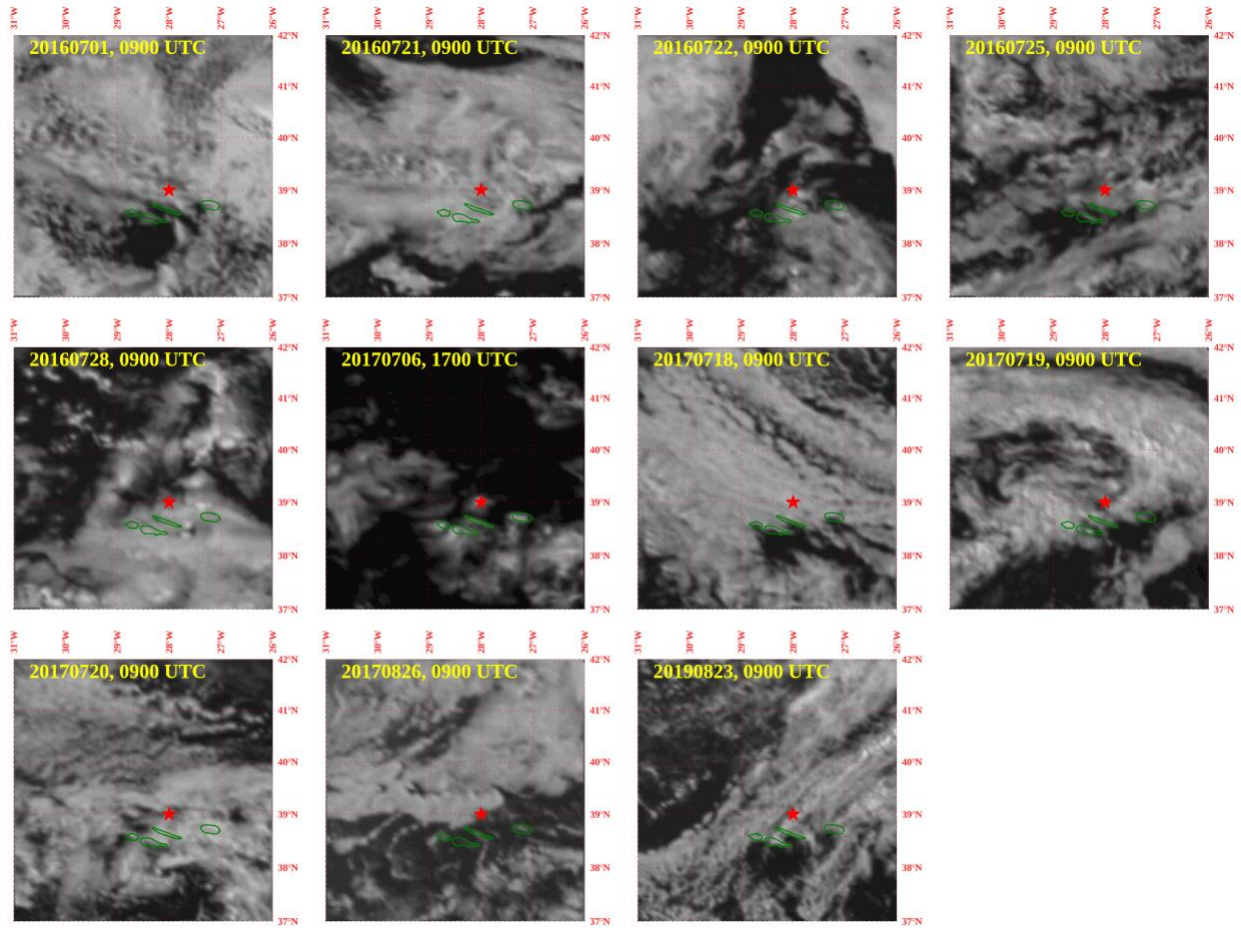


Figure S2. Cloud fields from Meteosat visible reflectance for the 11 cases at 09:00 UTC. For 6 July 2017, Meteosat observations were unavailable at 09:00 UTC; therefore, cloud fields at 17:00 UTC are shown instead.

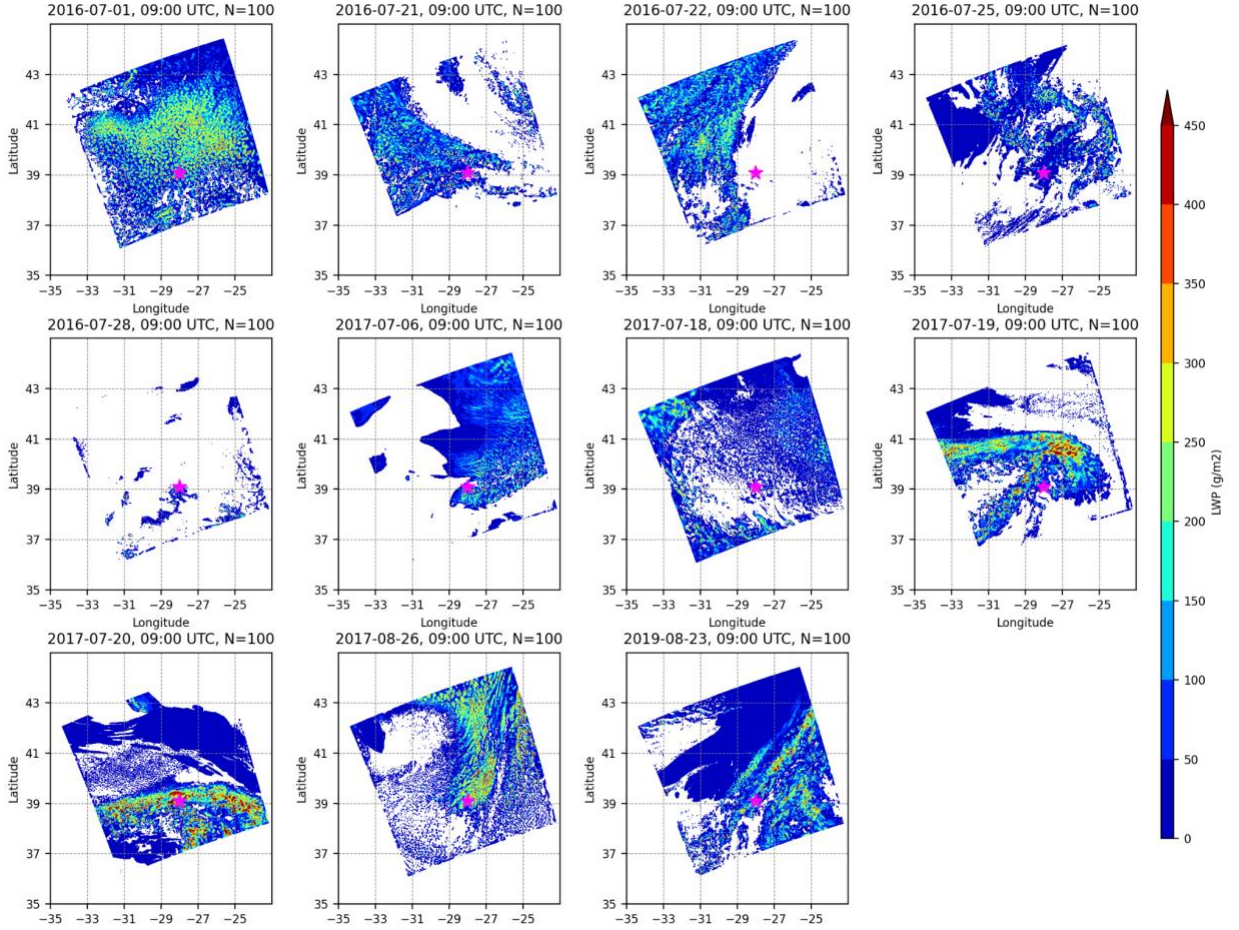


Figure S3. Simulated cloud liquid water path (LWP; units: gm^{-2}) for the clean experiment ($N=100\text{ cm}^{-3}$) at 09:00 UTC for all 11 cases.

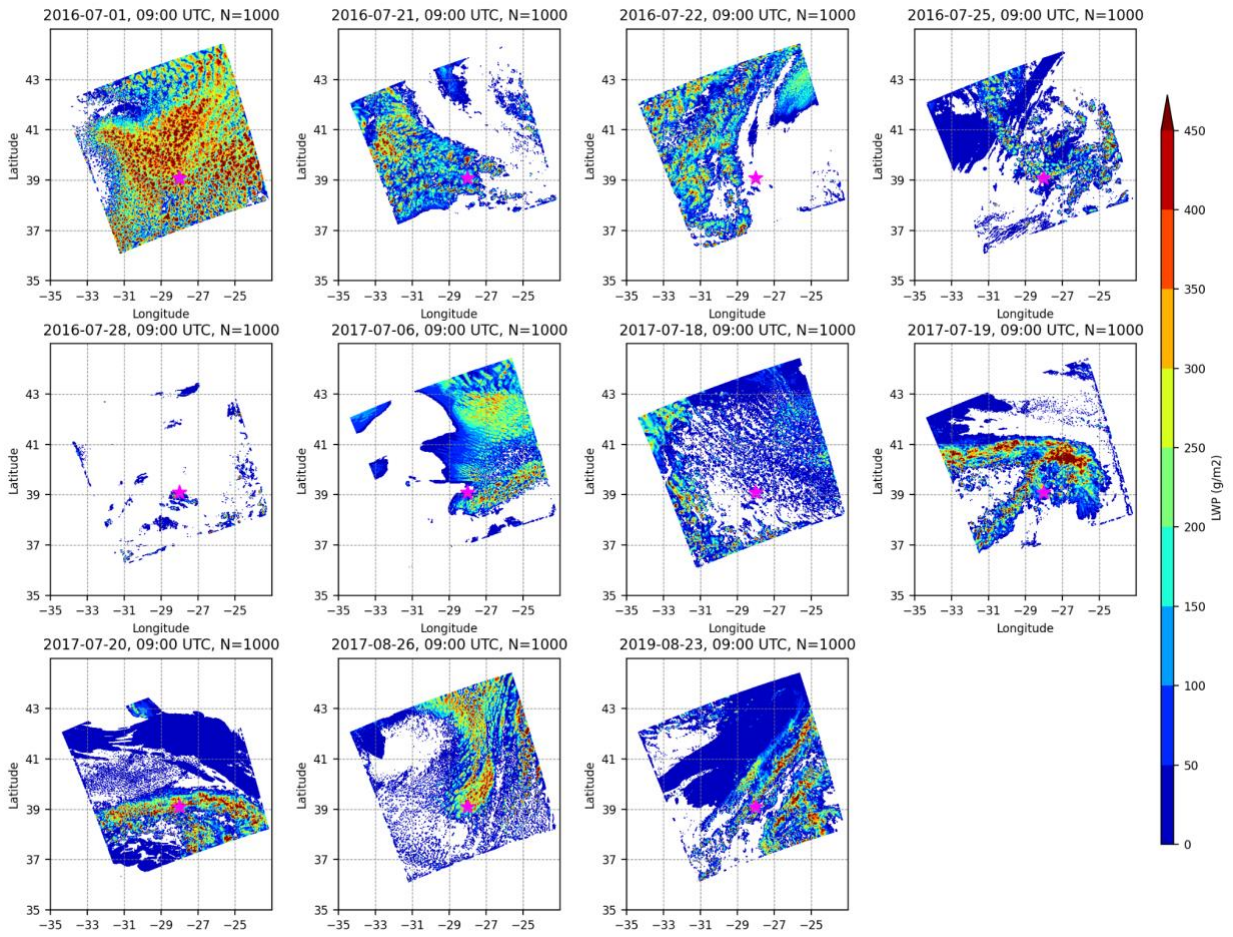


Figure S4. Simulated cloud liquid water path (LWP; units: gm^{-2}) for the polluted experiment (N=1000 cm^{-3}) at 09:00 UTC for all 11 cases.

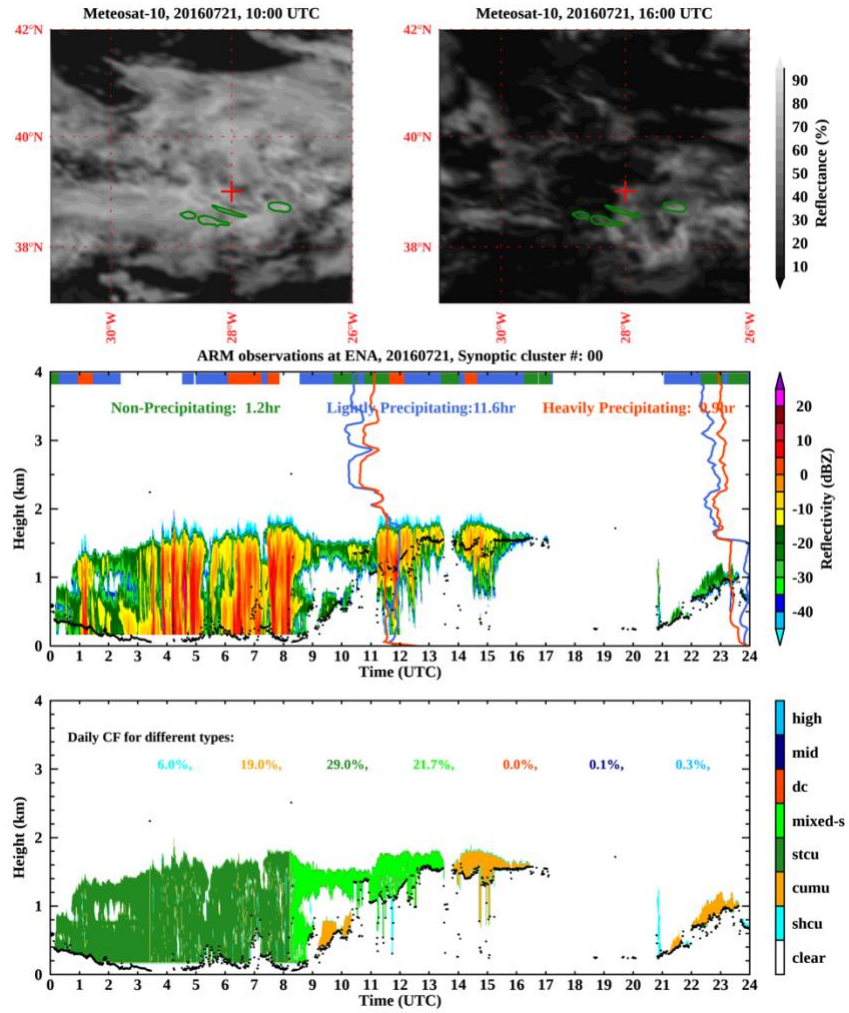


Figure S5. Cloud fields from Meteosat and ground-based radar observations on 21 July 2016. Top panels: Meteosat visible reflectance over a $5^\circ \times 5^\circ$ region centered at the ARM ENA site (red cross) at 10:00 and 16:00 UTC. Middle panels: radar reflectivity (contours) and best-estimated cloud base height (black dots) from the ARSCL product at the ARM ENA site, overlaid with temperature profiles (red lines) and specific humidity profiles (blue lines) from radiosonde observations. Bottom panels: cloud type classification based on cloud morphology. A detailed description of cloud-type classification method is provided in Zheng et al. (2025).

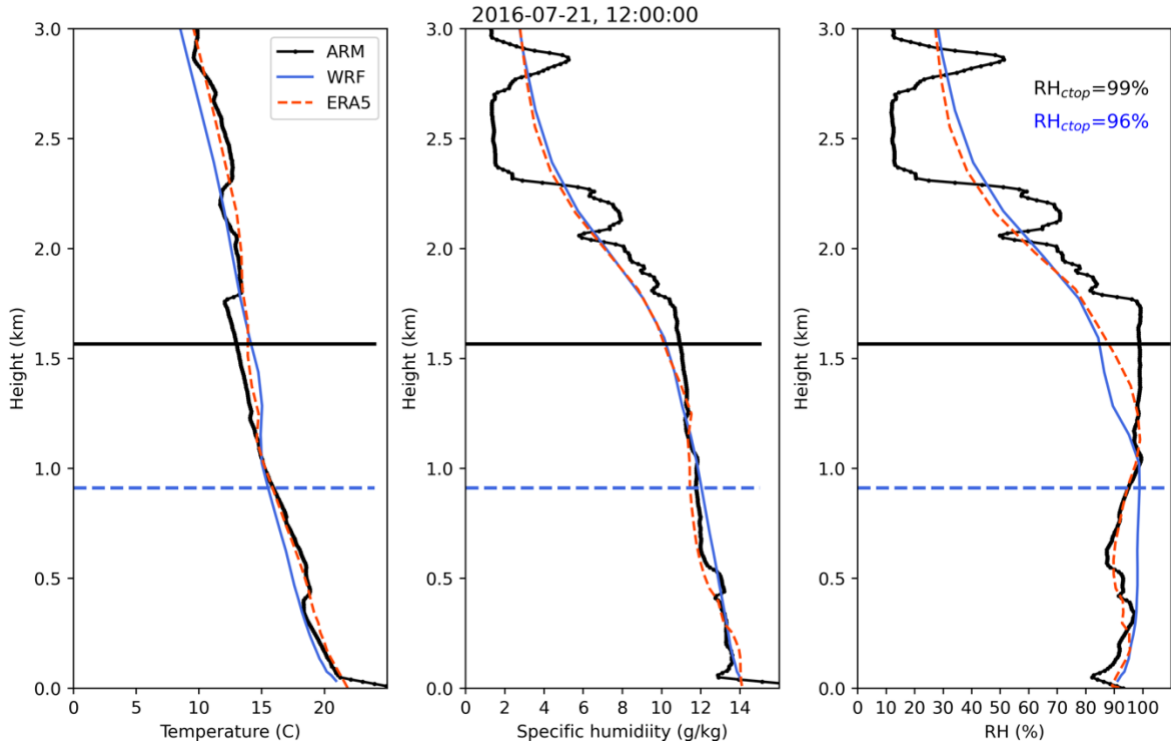


Figure S6. Thermodynamic profile of (a) temperature (b) specific humidity and (c) relative humidity from ARM radiosonde observations (black lines), WRF simulations (blue lines), and ERA5 reanalysis (red dashed lines) on 21 July 2016 at 12:00 UTC. The black solid and blue dashed horizontal lines indicate cloud-top heights derived from ground-based radar observations and WRF simulations, respectively.

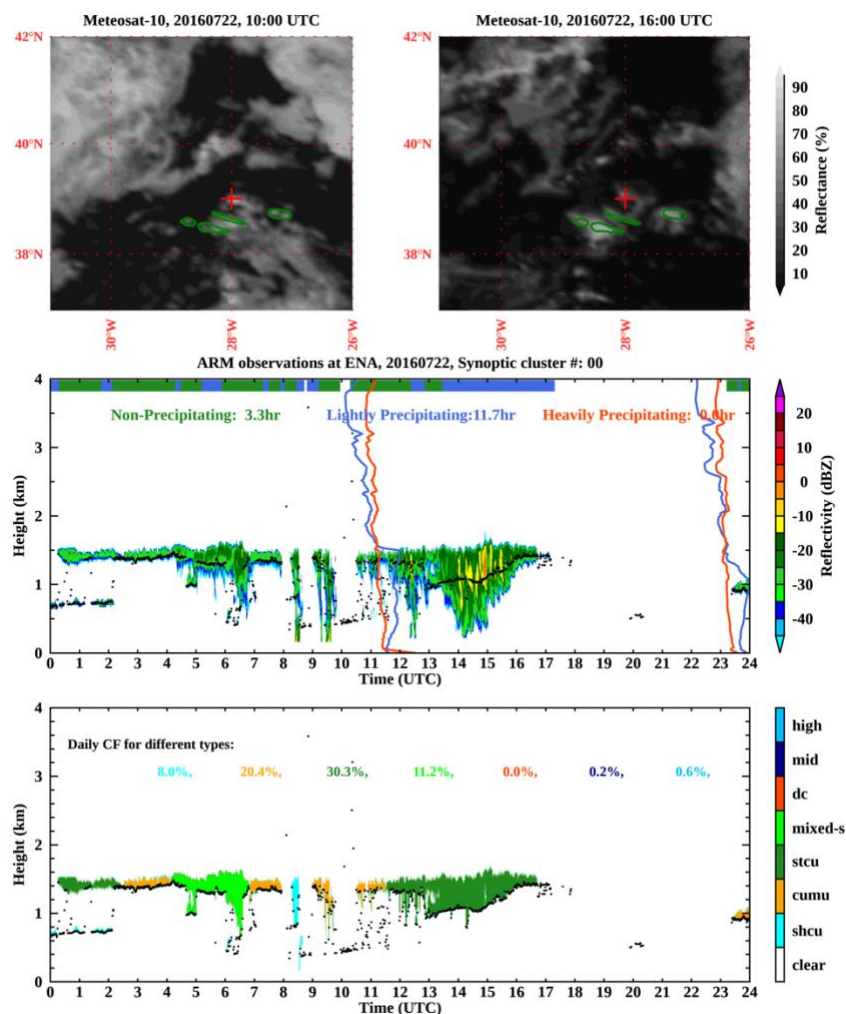


Figure S7. Same variables and layout as Figure S5, but for 22 July 2016. Top panels show Meteosat visible reflectance, middle panels show radar reflectivity with thermodynamic profiles, and bottom panels show classified cloud types.

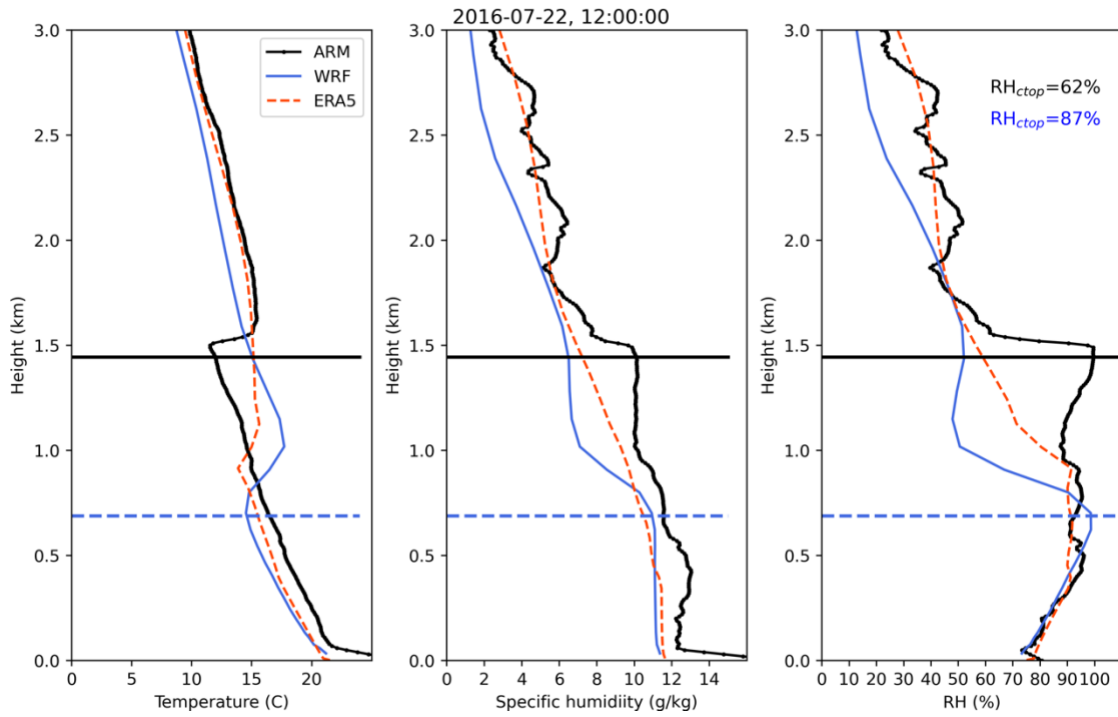


Figure S8. Thermodynamic profile of (a) temperature (b) specific humidity and (c) relative humidity from ARM radiosonde observations (black lines), WRF simulations (blue lines), and ERA5 reanalysis (red dashed lines) on 22 July 2016 at 12:00 UTC. The black solid and blue dashed horizontal lines indicate cloud-top heights derived from ground-based radar observations and WRF simulations, respectively.

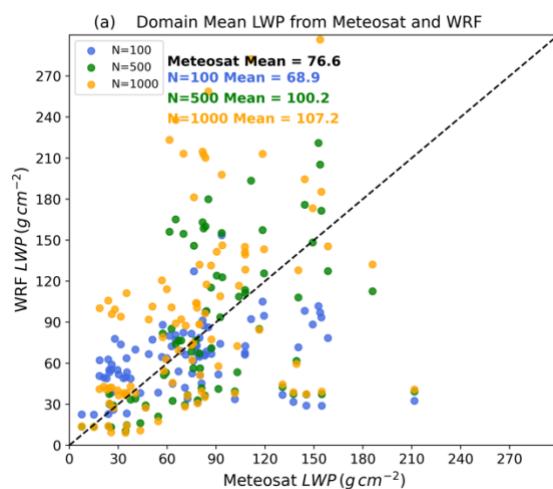


Figure S9: Scatter plot of domain-averaged cloud liquid water path (LWP) from Meteosat observations and WRF model simulation. Different colors represent different aerosol concentration experiments: N=100 (blue), N=500 (green), and N=1000 (orange).

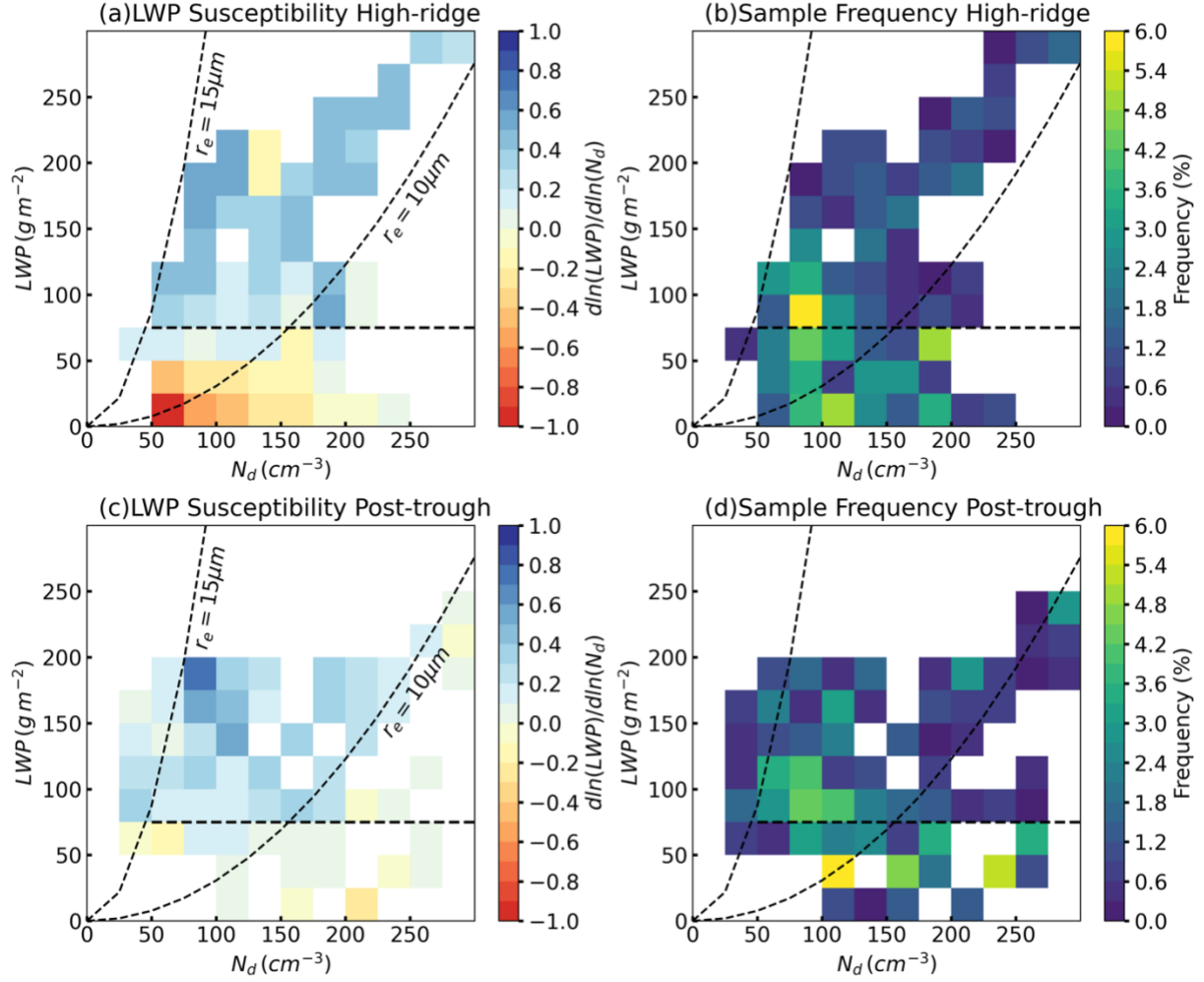


Figure S10. Mean liquid water path (LWP) susceptibility from WRF simulations under different synoptic regimes: (a, b) high-ridge regime and (c, d) post-trough regime. Panels (a) and (c) show cloud LWP susceptibility $d\ln(LWP)/d\ln(N_d)$, (b) and (d) show the frequency of occurrence in each bin. Dashed lines in each panel indicate thresholds of $r_e = 15 \mu m$, $r_e = 10 \mu m$ for precipitation, and LWP = $75 g m^{-2}$ for thick clouds. Precipitating clouds are located to the left of the $r_e = 15 \mu m$ line, and thick clouds are defined as LWP > $75 g m^{-2}$.